Journal of the Earth & Space Physics. Vol. 37, No. 1, 2011, P. 11-24

Analysis and Prediction of GNSS Estimated Total Electron Contents

Asgari, J.[1*] and Amiri-Simkooei, A. R.[2]

[1] *Assistant Professor, Department of Surveying Engineering, Faculty of Engineering, University of Isfahan, Iran*
[2] *Assistant Professor, Department of Surveying Engineering, Faculty of Engineering, University of Isfahan, Iran*

(Received: 13 Oct 2009 , Accepted: 20 Oct 2010)

Abstract

The least squares harmonic estimation is applied to the hourly time-series of Total Electron Contents (TEC) derived from ionospheric models using seven years of GPS observations processed by Bernese software. The frequencies of dominant spectral components in the spectrum are estimated. We observe significant periodic patterns with periods of 24 h and its fractions 24h/n, n=2,…,11, which are the well-known Fourier series decomposition of the diurnal periodic pattern of the ionospheric variations. The principal component with daily signal is due to the day-night variation of TEC values. The semidiurnal and tri-diurnal components can be explained by the substorm signatures in both auroral electrojet (in layer E) and ring current variations (related to magnetosphere at low latitudes) and tidal effects. Also, the spectrum shows the well-known 27-day period of solar cycle variations. We observe annual, semi-annual and tri-annual signals in the series. The detected signals are then applied to perform an ionospheric prediction. The results indicate that a substantial part (in the absolute sense) of the TEC values can be predicted using this base function, and an undetectable part remains as disturbed noise which can exceed 20 TEC units for the disturbed ionosphere. In comparison with the standard Klobuchar model, the model presented in this contribution will significantly improve the single frequency GPS positioning accuracy.

Key words: Ionosphere, Harmonic estimation, Total electron content (TEC), GPS, Global Navigation Satellite System

تحلیل و پیش‌بینی محتوای کلی الکترون (TEC) حاصل از مشاهدات سامانه ناوبری جهانی

جمال عسگری[۱] و علیرضا امیری سیمکویی[۲]

[۱] *استادیار، گروه مهندسی نقشه برداری، دانشکده فنی و مهندسی، دانشگاه اصفهان، ایران*
[۲] *استادیار، گروه مهندسی نقشه برداری، دانشکده فنی و مهندسی، دانشگاه اصفهان، ایران*

(دریافت: ۸۸/۷/۲۱ ، پذیرش نهایی: ۸۹/۷/۲۸)

چکیده

در این تحقیق از روش برآورد هماهنگ (هارمونیک) کمترین مربعات روی سری‌های زمانی یون‌سپهر (TEC) به طول زمانی هفت سال، که با استفاده از پردازش داده‌های GPS با نرم‌افزار Bernese محاسبه شده‌اند، استفاده شده است. بسامدهای طیفی مؤلفه‌های اصلی برآورد شده‌اند. در این طیف‌ها دوره 24 h و کسرهای آن ,24h/n که n=1,2,…,11 مشاهده می‌شوند که تجزیه معروف سری فوریه از تغییرات روزانه یون‌سپهر هستند. عامل اصلی این سیگنال روزانه تغییرات شبانه‌روزی TEC است. مؤلفه های نیم‌روزانه و ثلث‌روزانه می‌تواند به‌دلیل ردپای substorm ها به دو صورت حرکات قطبی ذرات باردار (در لایه‌ی E) و تغییرات در جریان حلقوی (مرتبط با میدان الکتریکی مغناطیس‌سپهر در عرض‌های پایین) و همچنین تاثیرات کشندی (جذرومدی) باشد. همچنین طیف با دوره شناخته شده ۲۷ روز نیز به‌دست آمده که مرتبط با نوسان‌های دوره‌ای خورشیدی است. علاوه‌براین، دوره‌های سالانه، نیم‌سالانه و ثلث‌سالانه نیز مشاهده می‌شود. درنهایت، از دوره‌های به‌دست آمده برای ایجاد یک الگوی پیش‌بینی یون‌سپهری استفاده

[*]Corresponding author: Tel: 0311-7934020 Fax: 0311-7932675 E-mail: jamal.asgari@gmail.com

شده است. نتایج نشانگر آن است که بخش قابل‌ملاحظه‌ای (به‌طور مطلق) از مقادیر TEC با این توابع پایه قابل پیش‌بینی است، و قسمت غیرقابل کشف که به‌صورت نوفه آشفته باقی می‌ماند می‌تواند در حالت یون‌سپهر آشفته تا 20TECU برسد. در مقایسه با مدل استاندارد Klobuchar این روش به صورت معناداری دقت تعیین موقعیت با GPS تک بسامدی را افزایش خواهد داد.

واژه‌های کلیدی: یون‌سپهر، برآورد هماهنگ (هامورنیک)، TEC، GPS

1 INTRODUCTION

The existence of the ionosphere is directly related to radiation emitted from the sun. The relative configuration of the Earth with respect to the sun is responsible for a large part of the variations in the ionosphere. The ionospheric variations are classified as regular and irregular variations. Regular variations occur more or less in cycles and therefore, can be predicted in advance with reasonable accuracy. Examples of regular variations are diurnal, seasonal, and solar cycle variations (Jain et al. 1996). The irregular variations are of abnormal behavior of the sun and therefore, cannot be predicted in advance.

The daily rotation of the Earth around its axis is responsible for a large part of the daily variations in the ionosphere. Daily variations in the ionosphere are a result of the 24-hour rotation of the Earth about its axis. Ionization depends on the angle of the sun, which is greatly reduced at night. The principal component (24 hours) with daily signal is due to the day-night variation of TEC values. The existence of semidiurnal and tri-diurnal periods is explained by Pi et al. (1993) and Oyekola et al. (2006). The former explains that the daytime double maxima (twin peaks or bite-outs) in the ionospheric total electron content (TEC) at middle and lower latitudes are due to substorm signatures in both auroral electrojet and ring current variations. They show that the diurnal double maxima in TEC can be created by a combined effect of E × B drift and altitude-dependent F region chemical loss. There exists another double maxima phenomenon on the latitude profile near the maximum ionospheric effect (latitude profile at zero longitude on sun-fixed frame) that is due to equatorial anomaly (Oliveira et al. 2005).

Examples of the network estimated daily TEC values are superposed for several points of the French Permanent GPS network (Fig. 1). There are two peaks for all of the estimated daily TEC values in this sketch. The latter explains the effects of tides on the upper ionosphere. But the exact interpretation is rather difficult due to its weak spectral component. Some other components are reported in a research using atmospheric radar (Balan, et al. 2006).

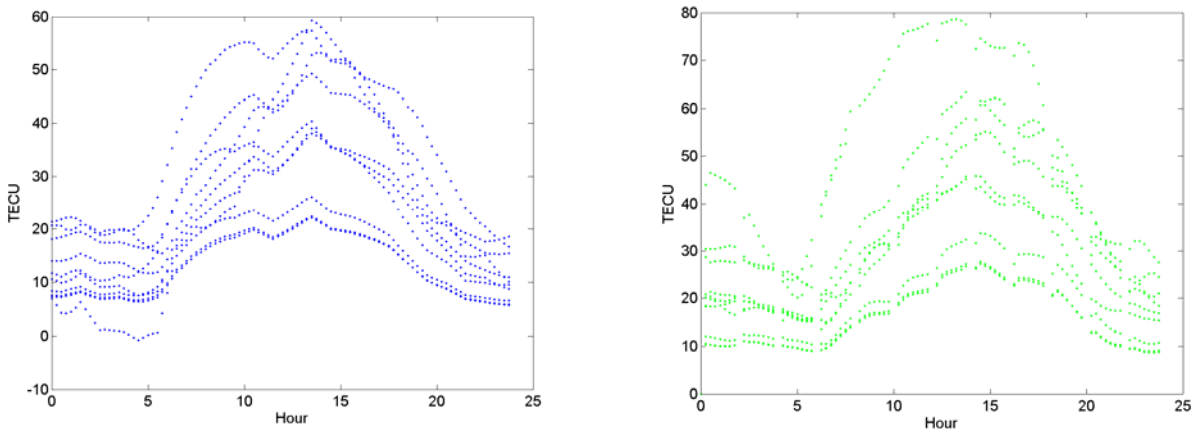

Figure 1. The ionospheric diurnal double maxima; local ionospheric model (left), CODE global model (right).

Seasonal variations are the result of the Earth revolving around the sun; the relative position of the sun moves from one hemisphere to the other with changes in seasons. Seasonal variations of the ionospheric layers correspond to the highest angle of the sun. Therefore, the ionization density of the layers is greatest during the summer. The F2 layer, however, does not follow this pattern; its ionization is greatest in winter and least in summer. As a result, operating frequencies for F2 layer propagation are higher in the winter than in the summer.

The sunspots are partly responsible for variations in the ionization level of the ionosphere. Sunspots can occur unexpectedly. A regular solar cycle variation of sunspot activity has a minimum and maximum level and occurs approximately every 11 years. The sunspot distribution at the solar surface is not homogeneous. Solar rotation with an approximate period of 27 days is also reflected in sunspot numbers (Le Mouël et al. 2007). The number of sunspots at any given time is continually subject to change as some disappear and new ones emerge.

Ionospheric estimation using GNSS systems becomes one of the routine methods for TEC derivation. Different models including single layer (Schaer 1999), tomographic (Artru 2001), and four dimensional (Memarzadeh 2009), have been used for TEC representation. The continuous nature of permanent GPS stations and the long time span of data are the main advantages of this method for ionospheric estimation. The harmonic analysis of global TEC models was previously employed by Schaer (1999) and Unnikrishnan et al. (2002). The application of this data for TEC modeling and prediction is one of the main objectives of this research.

The frequency dependence of the ionospheric effect is a tool for measuring the Total Electron Content (TEC) in the ionosphere (Schaer 1999). Using GPS permanent station arrays, it is possible to estimate global or local ionospheric models (Artru 2001). Since the TEC values show cyclic variations for their regular part, they can be modeled by a series of periodic functions—sinusoidal functions for instance. We apply the least squares harmonic estimation (LS-HE), developed by Amiri-Simkooei 2007, to the TEC values derived from ionospheric models. The time series in our analysis consists of TEC values computed from ionospheric models using GPS observations in the French Permanent GPS Network (RGP). Seven years (2001 to 2007) of hourly ionospheric data are analyzed using LS-HE.

This analysis gives us the possibility of proposing a model which takes into account a longer data set. The model gives the standard deviation of TEC prediction to be in the order of 5 TECU (TEC Unit). Despite high scintillations, the model gives reliable results because it is based on real data from local networks.

2 HARMONIC ESTIMATION

In GPS data processing, one usually starts with formulating a system of observation equations, which consists of two models: the functional model and the stochastic model. The functional model captures all functional effects, while the stochastic model captures all stochastic effects. We now consider the functional model and present the formulation of the least-squares harmonic estimation applied to the linear model of observation equations

$$\mathrm{E}(y)=Ax,\ \mathrm{D}(y)=Q_y \qquad (1)$$

where A is the $m\times n$ design matrix, Q_y is the $m\times m$ covariance matrix of the m-vector of observables y, x is the n-vector of unknown parameters, and E and D are the expectation and dispersion operators, respectively.

We use the harmonic estimation method to identify and hence compensate for unmodelled periodic effects in the functional part of the model. Consider the model of observation equations $E(y)=Ax$, where the time series $y=[y_1, y_2, ..., y_m]^T$ is also

expressed as a periodic pattern. We may assume that y can be expressed as an individual trigonometric term as $y_i = a_k \cos\omega_k t_i + b_k \sin\omega_k t_i$ (a sinusoidal wave). In the matrix notation, when including the functional part Ax of the model, one obtains

$$E(y) = Ax + A_k x_k, \quad D(y) = Q_y \tag{2}$$

where the matrix A_k consists of two columns corresponding to frequency ω_k of the sinusoidal function

$$A_k = \begin{bmatrix} \cos\omega_k t_1 & \sin\omega_k t_1 \\ \cos\omega_k t_2 & \sin\omega_k t_2 \\ \vdots & \vdots \\ \cos\omega_k t_m & \sin\omega_k t_m \end{bmatrix}, \quad x_k = \begin{bmatrix} a_k \\ b_k \end{bmatrix} \tag{3}$$

with a_k, b_k and ω_k being unknown real numbers. The problem of finding the unknown frequency ω_k in Eq. (2) is the task of harmonic estimation. For this purpose the following null and alternative hypotheses are put forward: $H_0: E(y) = Ax$ versus $H_a: E(y) = Ax + A_k x_k$, where under the null hypothesis the periodic effect is absent, while under the alternative hypothesis it is present (i.e. it is significant). The identification and testing of the frequency ω_k is completed through the following steps:

The frequency ω_i (and correspondingly A_i) identified by solving the minimization problem

$$\omega_k = \arg\min_{\omega_j} \| P^{\perp}_{[A\ A_j]} y \|^2_{Q_y^{-1}} \tag{4}$$

where $P^{\perp}_{[.]} = I - [.]([.]^T Q_y^{-1}[.])[.]^T Q_y^{-1}$ is an orthogonal projector (under the alternative hypothesis). The matrix A_j has the same structure as A_k in Eq. (3); the one that minimizes the preceding criterion is set to be A_k. An equivalent expression of the above minimization problem is expressed as the following maximization problem (Amiri-Simkooei 2007):

$$\omega_k = \arg\max_{\omega_j} P(\omega_j) \tag{5}$$

where

$$P(\omega_j) = \hat{e}_0^T Q_y^{-1} A_j (A_j^T Q_y^{-1} P_A^{\perp} A_j)^{-1} A_j^T Q_y^{-1} \hat{e}_0 \tag{6}$$

with $\hat{e}_0 = P_A^{\perp} y$ the least-squares residuals and $P_A^{\perp} = I - A(A^T Q_y^{-1} A) A^T Q_y^{-1}$ an orthogonal projector (both are given under the null hypothesis). Analytical evaluation of the above maximization problem is complicated. In practice, one has to be satisfied with numerical evaluation. A plot of spectral values $P(\omega_j)$ versus a set of discrete values for ω_j can be used to investigate the contribution of different frequencies in the construction of the original data series y. In other words, we may compute the spectral values for different frequencies ω_j using Eq. (6) and take the frequency at which $P(\omega_j)$ achieves its maximum value. This is considered to be ω_k from which the matrix A_k is constructed using Eq. (3).

After obtaining ω_k, one has to test H_0 against H_a to see whether the detected frequency is indeed significant. The following test statistic can be used

$$P(\omega_k) = \hat{e}_0^T Q_y^{-1} A_k (A_k^T Q_y^{-1} P_A^{\perp} A_k)^{-1} A_k^T Q_y^{-1} \hat{e}_0 \tag{7}$$

Under H_0, the test statistic has a central chi-square distribution with two degrees of freedom

$$T_2 \sim \chi^2(2,0) \tag{8}$$

Where the covariance matrix is of the form $Q_y = \sigma^2 Q$, with σ^2 the unknown variance of unit weight, the test statistic as well as its distribution will be modified (see Amiri-Simkooei, 2007). If the null hypothesis is rejected, we may perform the same procedure for finding yet another frequency.

As a generalized form of the Fourier Spectral Analysis, this method is neither limited to evenly spaced data nor to integer frequencies. As a special case, consider a zero-mean stationary random process. We then have, $A = 0$, and hence $P_A^{\perp} = I$. If, in addition, the noise of the random process is only white, we may write $Q_y = I$. Equation (6) then simplifies to

$$P(\omega_j) = \hat{e}_0^T A_j (A_j^T A_j)^{-1} A_j^T \hat{e}_0 \quad (9)$$

which is identical to the least-squares spectral analysis (LSSA) method developed by Vaníček (1971). For some applications we refer to (Craymer 1998; Abbasi 1999; Asgari and Harmel 2005).

Our application of harmonic estimation is to find any potential periodicities in the non-equally spaced time-series of the TEC values derived from ionospheric models. There are periodic components to the solar variations, the principal one being the 11.3-year solar cycle (or sunspot cycle). The TEC values exhibit this period. Other important signals detected by harmonic estimation are the annual and diurnal signals, possibly along with their higher-order harmonics. The detected frequencies will be used to predict the TEC values for the last days of the series. This gives an indication that only 80% of the ionospheric errors can be modeled and a 20% portion remains undetectable as disturbed noise.

3 PRE-PROCESSING OF GPS DATA

Ionospheric delay estimation using GPS data

GPS signals pass through different layers of the atmosphere. The effect of ionospheric layers on GPS signals depends on signal frequency and the Total Electron Content (TEC). This effect ranges from a few meters to tens of meters. In the high solar activity this value could reach more than 100 meters. Due to the irregular variations it is impossible to totally determine the TEC value using a deterministic model. Klobuchar ionospheric parameters, broadcast from GPS satellites, can correct only about 50% of the ionospheric effect (Klobuchar 1987; Seeber 2003).

The frequency dependence of GPS signals travel time in the ionosphere is employed to extract the ionospheric delay. The Geometry-free GPS observations are the basis of TEC estimations. The L4 observable is expressed as (Schaer 1999)

$$L_4 = L_1 - L_2$$

$$L_4 = -\alpha\left(\frac{1}{f_1^{\,2}} - \frac{1}{f_2^{\,2}}\right) M_1(z)\, E(\beta, s) + \lambda_1 N_1 - \lambda_2 N_2 + \varepsilon \quad (10)$$

where $\alpha = 4.03\, ms^{-2} TECU^{-1}$, L_1 and L_2 are the GPS phase observables, f_1 and f_2 are the L_1 and L_2 frequencies respectively, $M_1(z)$ is the mapping function, $E(\beta, s)$ is the vertical TEC value, β is the geographical or geomagnetic latitude, s is the sun-fixed longitude, N_1 and N_2 are the initial phase ambiguities of L_1 and L_2, λ_1 and λ_2 are the wavelength of L_1 and L_2.

Single layer and tomographical models using permanent GPS networks have been extensively investigated and applied (Schaer 1999; Artru 2001; Hernández-Pajares 2000). All of these models are based on the estimation of TEC using discrete GPS observations. But by applying the appropriate base functions, one may obtain ionospheric models in continuous domain. The estimated TEC of French Permanent GPS Network (RGP) is modeled either by polynomial base functions, which are useful for local modeling of the ionosphere, or by spherical harmonics. The local TEC model is represented by the following Taylor series for vertical TEC value E_v (Dach et al. 2007)

$$E_v(\beta, s) = \sum_{n=0}^{n_{\max}} \sum_{m=0}^{m_{\max}} E_{nm} (\beta - \beta_o)^n (s - s_o)^m \quad (11)$$

where $n_{\max}$ and $m_{\max}$ are the degrees of the Taylor series, s_o and βo are the origin of Taylor series development, E_{nm} are the unknown coefficients, and β and s are the latitude and sun-fixed longitudes of the pierce point, respectively.

The global TEC model based on spherical harmonics expansion is given as (Dach et al 2007)

$$E_v(\beta,s)=\sum_{n=0}^{n_{\max}}\sum_{m=0}^{n}\tilde{P}_{nm}\sin(\beta)(a_{nm}\cos(m\,s)+b_{nm}\sin(m\,s)) \quad (12)$$

where $n_{\max}$ is the maximum degree of spherical harmonic expansion, $\tilde{P}_{nm}$ is the normalized Legendre function of degree n and order m, and a_{nm} and b_{nm} are the unknown TEC parameters. This model can be used both in global and in regional scales.

Extraction of ionospheric data series

In this section we explain our methodology to extract the time series of the TEC values for further analyses using least-squares harmonic estimation (LS-HE). The data corresponds to ionospheric models derived from Réseau GPS Permanent (RGP) stations (http://rgp.ign.fr/PRODUITS/iono.php). The RGP network consists of 23 permanent stations in mid 2001, and increases to about 140 stations at the end of 2007. There exist more than 60,000 hourly TEC values for the time series.

Hourly local TEC model coefficients are used as the data series of our analyses. E_{oo} represents the TEC value at the point of development and has the most important contribution in the Taylor series. The global number of ionospheric electrons could be deduced from a_{oo} (the constant term in Eq. 12) in the global model when the development is performed over the whole Earth (Schaer 1999). It then makes the data series used in the least-squares harmonic estimation (LS-HE) method.

The problem arises when comparing different hourly solutions using E_{oo}, because the origin of the Taylor series development varies for every hourly ionospheric model (about several degrees). In the following we propose a method to change the origin of development and to unify the point of development for all hourly solutions. After applying this idea, an identical origin for all local TEC models (Taylor series) is obtained.

The second degree polynomial model has the following form:

$$\begin{aligned} TEC &= E_{00}+E_{01}\Delta s+E_{02}\Delta s^2+\\ &E_{10}\Delta\beta+E_{11}\Delta\beta\Delta s+E_{20}\Delta\beta^2\\ &\Delta\beta=\beta-\beta_o\\ &\Delta s=s-s_o \end{aligned} \quad (13)$$

We now change the origin from β_o and s_o to β_o' and s_o' in order to obtain a unique point of development

$$\beta_o'=\beta_o+d\beta_o$$

$$s_o'=s_o+ds_o$$

Therefore, after applying this transformation, β_o' and s_o' become constant over the entire time series. One then obtains

$$\Delta\beta'=\beta-\beta_o'=\Delta\beta-d\beta_o$$

$$\Delta s'=s-s_o'=\Delta s-ds_o$$

Equation (13) can then be reformulated as

$$\begin{aligned} TEC &= E_{00}+E_{01}(\Delta s'+ds_o)+\\ &E_{02}(\Delta s'+ds_o)^2+E_{10}(\Delta\beta'+d\beta_o)+\\ &E_{11}(\Delta\beta'+d\beta_o)(\Delta s'+ds_o)+E_{20}(\Delta\beta'+d\beta_o)^2 \end{aligned} \quad (14)$$

Rearranging the above equation gives the Taylor series with a new origin. For example, the constant term E_{oo}' becomes

$$\begin{aligned} E_{00}' &= E_{00}+E_{01}ds_o+E_{02}ds_o^2+\\ &E_{10}d\beta_o+E_{11}ds_o d\beta_o+E_{20}d\beta_o^2 \end{aligned} \quad (15)$$

Other coefficients can be computed in a similar manner. The following transformation is used to obtain the new coefficients:

$$E'=E\,M \quad (16)$$

where E is the old coefficient vector and E' is the new coefficient vector

$$E=[E_{00}\,E_{01}\,E_{02}\,E_{10}\,E_{11}\,E_{20}],$$

$$E'=[E_{00}'\,E_{01}'\,E_{02}'\,E_{10}'\,E_{11}'\,E_{20}'],$$

and M is the transformation matrix

$$M=\begin{bmatrix} 1 & 0 & 0 & 0 & 0 & 0\\ ds_o & 1 & 0 & 0 & 0 & 0\\ ds_o^2 & 2ds_o & 1 & 0 & 0 & 0\\ d\beta_o & 0 & 0 & 1 & 0 & 0\\ ds_o d\beta_o & 0 & 0 & 2d\beta_o & 1 & 0\\ d\beta_o^2 & d\beta_o & 0 & ds_o & 0 & 1 \end{bmatrix}$$

In a similar manner the Taylor series expansion can be used to change the origin of the third-degree polynomial models, which corresponds to data from 2005 to 2007. After transforming all of the hourly data, we obtain new Taylor series for each hourly data. Note that irregular gaps exist in the data set. Figure 2 shows the plot of E'_{oo} over the period 2001 to 2007, which represents the TEC values of the origin of the expansion.

4 RESULTS AND dISCUSSIONS

Harmonic analysis and interpretation

We now apply the LS-HE to the non-equally spaced time-series of TEC values of the previous section. Numerical search for the discrete frequencies is applied to Eq. (7). The step size used for the periods $T_j=2\pi/\omega_j$ is small at high frequencies and gets larger at lower frequencies. The following recursive relation is used:

$$T_{j+1}=T_j\left(1+\frac{\alpha T_j}{T}\right),\quad \alpha=0.1,\ j=1,2,... \tag{17}$$

with a starting period of $T_1=2$ hours (Nyquist period) and T being the total time span of 56395 hours (2350 days). For this time series, the lowest frequency checked in the analysis is $\omega_{\min}=2\pi/T$, i.e. one cycle over the total time span. To avoid a $A_j^T P_A^{\perp} A_j$ singularity, one needs to exclude the previously detected frequencies $\omega_1,...,\omega_{i-1}$ in the spectrum when finding ω_i .

The harmonic analysis is applied to the TEC values to obtain the least-squares spectrum of the series and to interpret the results. Figure 3 is the result for the frequency spacing of α=0.1 in Eq. (17). The periods with dominant spectral values are from 2 hour to one day; the spectrum shows a periodic pattern with periods of 24h/n, n=1,…,11. The most important components have the periods of 1, 1/2, and 1/3 day.

A zoom-in of the daily signals is shown in Fig. 4, when the time-series of TEC values has been split into two parts. Peaks are evident at harmonics of 1 cycle per day (cpd) up to 11 cpd. To explain these signals we recall the theory of Fourier series expansion of periodic functions. Let the function $f(x)$ be a periodic function with period of T (i.e. $f(x)=f(x+T)$). Such a function can be written as an infinite sum of sine and cosine functions on the interval [-T/2, T/2]. The results presented are in fact an interesting example of a Fourier series decomposition of a periodic function of $T=24$ hours into a truncated sum of simple oscillating functions sines and cosines. All of the individual components of such decomposition do not necessatily have a known underlying physical interpretation.

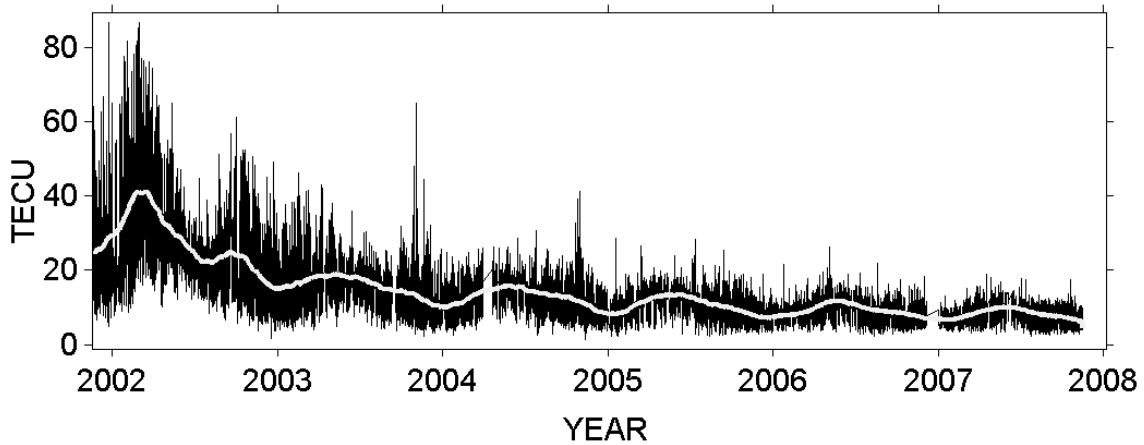

Figure 2. Hourly TEC values of 2001-2007 period for s=3o and β=45o (point of expansion) and moving averaged TEC values (bold gray line).

The one day period is the most natural period because of the day-night variation of the TEC values. This is the only component that is present in the standard Klobuchar model, which is expected to absorb only 50% of the effect (Seeber, 2003). The next two low periods with important spectral value are the semi-diurnal and tri-diurnal periods. Parts of such variations are due to movement of ionospheric plasma phenomenon caused by **E×B** drift explained in Pi et al. (1993). Figure 1 illustrates the diurnal double maxima obtained from the network estimated daily TEC values, which are superposed for several points of the network. Also, Fig. 5 (left frame) illustrates the bimonthly averaged TEC values over the whole data set in 2004, 2005, 2006, and 2007. The double-maximum phenomenon is clear in parts of the data set. In addition, parts of the variations of the semi-diurnal and tri-diurnal periods can likely be captured by tidal effect on the upper ionosphere as explained by Oyekola et al. (2006).

We now explain the most important seasonal variations of the TEC values. From the least-squares spectrum in Fig. 3, the most obvious cycle is around a period of 365 days, which is the well known annual cycle and results from the changing of the solar zenith angle (and hence solar radiation) through the year. The next peak occurs near 183 days, or semiannual signal as the first harmonic of the annual cycle. This variation is explained due to seasonal variation of the F2 region (Mansillaa et al. 2005). This variation is also clear in the raw data (Fig. 2). Total F_2 ionization is actually lower in the local summer months than in the winter (Seeber 2003). This effect is known as the winter anomaly. The anomaly is always present in the northern hemisphere, but is usually absent in the southern hemisphere during periods of low solar activity. Also, we observe the second harmonic (122 days) of the annual cycle.

There are signals with the solar cycle variation. The important period of 11.3 years is not detected because the data is not long enough. But the raw data exhibits this variation clearly (Fig. 2). Its physical reason is due to the solar high activity period. Quasi-periodicities near the solar-rotation period (27-day period) appear in the time series of TEC values. The signals with periods of 27.5, 23.74, 26.84, 28.88 days along with first harmonics can be seen in the spectrum (Fig.6). Note that the number of sunspots at any given time is not constant and changes with time.

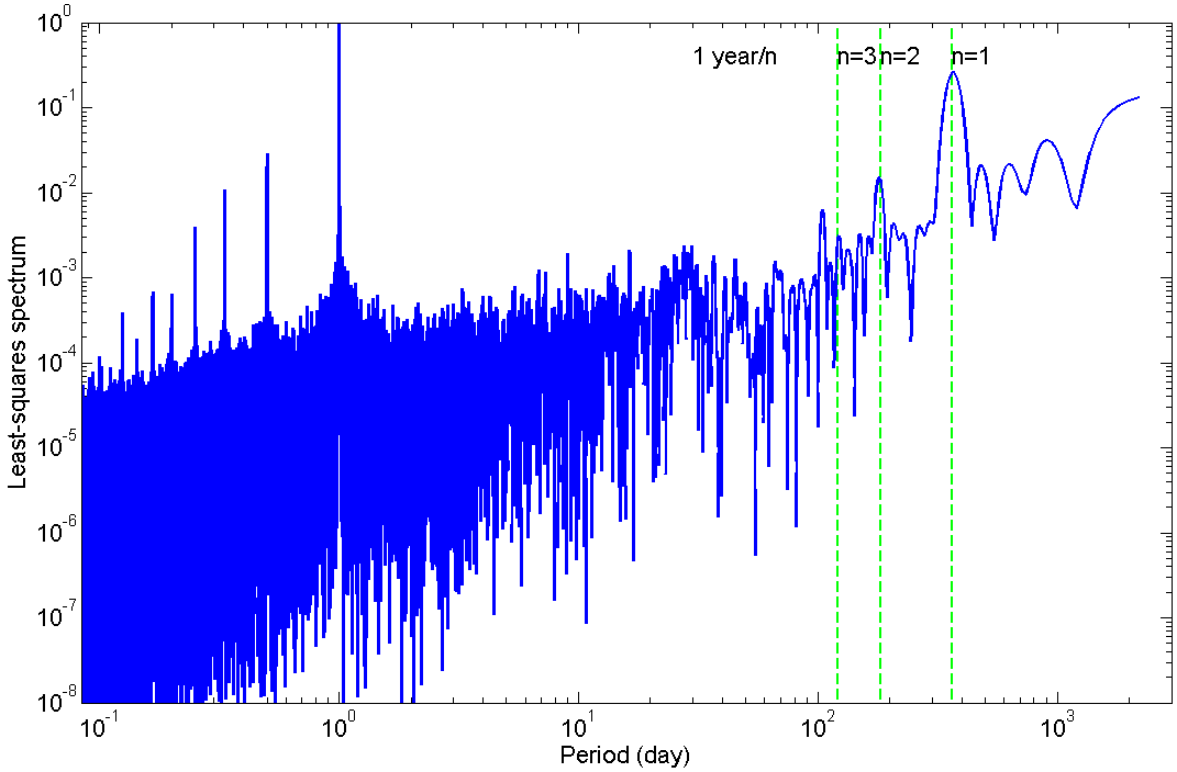

Figure 3. Least-squares spectrum of TEC values E'OO for 2001-2007 data; vertical dashed lines indicate annual signal and its first and second harmonic.

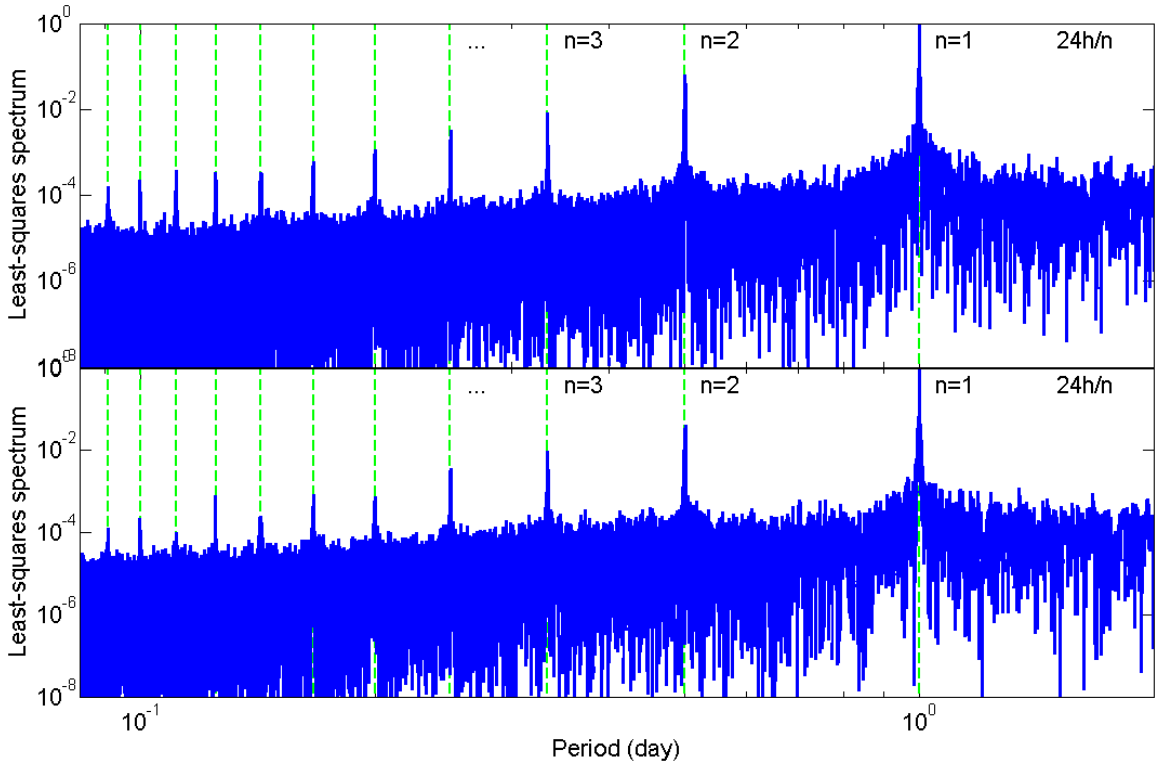

Figure 4. Zoom-in of least-squares spectrum for TEC values of lower period part; data set of 2001-2003 (top) and data set of 2004-2007 (bottom); vertical dashed lines indicate daily signal (24/n, n=1) and its higher order harmonics up to n=11.

5 TEMPORAL AND SPATIAL PREDICTION

Bimonthly averaged diurnal variations of the modeled TEC values (using harmonic functions) are shown in Fig. 5 (right). The modeled values match well with the bimonthly averaged values of the original data (left). Figure 7 shows the TEC values along with their modeled values over 2005 and 2006. It is concluded that only a contribution of 80% is captured by harmonic functions and a contribution of 20% remains undetected as ionospheric disturbed noise, which can reach up to 20 TEC units.

We now apply the detected periods to construct a harmonic prediction model. This model may contain from several hours of data to several weeks. But enlarging the time span of the data causes a greater prediction error. An example of such a model is given in Fig. 8. The model is based on the 3-day observed TEC values with previously detected harmonic signals. The degradation of the prediction is clear after several hours but the model is more consistent for the foregoing days. Based on our results, the method presented in this contribution can absorb about 80% of the ionospheric variations (a comparison between observed and modeled TEC values could reach this conclusion). This can be a significant improvement on the classical Klobuchar model which removes 50% of the ionospheric effects (Seeber, 2003, page 311).

It is important to note that this harmonic modeling is not capable of capturing the ionospheric scintillations. Figure 9 illustrates the spectrum for the harmonic trend removal from three days of TEC values. The spectrum shows that after removing each harmonic term, the corresponding peak in the spectrum will be removed. This is not however the case for longer time spans because the variation on the amplitude of the TEC does not permit the complete removal of the signal. This is mainly due to the seasonal and solar cycle

variation of the daily component.

The prediction scheme may be expanded from the time domain to the space domain. An ionospheric grid is formed using the LS-HE method. The TEC values, computed with the local TEC model, for several days of a regular grid are used for this purpose. The detected dominant frequencies are used for each point of the grid and a model is estimated. In other words, the algorithm described in Fig. 9 is now applied to all of the grid points. To predict the TEC values at the grid nodes, it is sufficient to extrapolate these functions for the desired time. Data from 53338.5 MJD to 53345.5 MJD are used for this numerical test. The prediction functions for the grid points are estimated. Figure 10 shows the predicted TEC values four hours after the observation time span. The overall agreement is in the order of 2-3 TECU. The prediction is quite satisfactory for a few hours after observation. Note that the prediction degrades when the predicted point is far from the network region.

It should be noted, however, that the path of different GPS satellite rays, traversing the ionosphere enlarge the effective region of ionospheric estimation from GPS observations. It means that not only does the ionosphere above the network contribute to the TEC estimation but also the distant regions of the ionosphere in part do so.

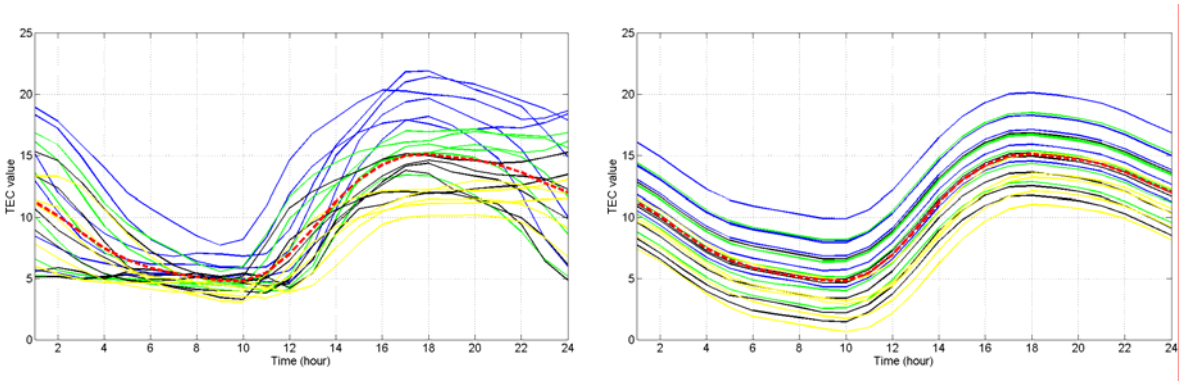

Figure 5. Bimonthly averaged diurnal variations of TEC values over 2004 (blue), 2005 (green), 2006 (black), and 2007 (yellow); dashed red line indicates average over entire time series; raw data (left) and modeled using harmonic functions (right).

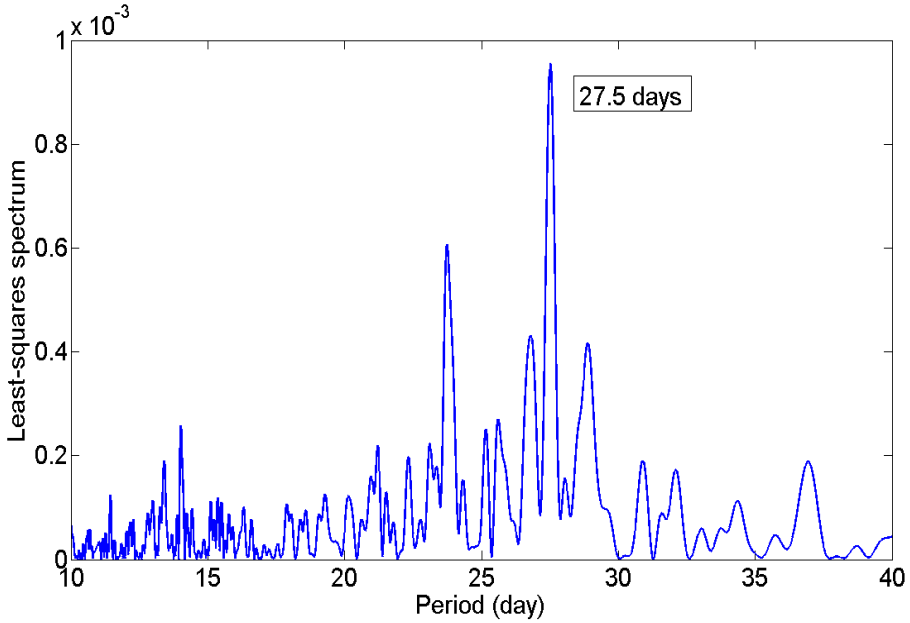

Figure 6. Zoom-in spectrum (linear scale) for periods of around one month related to solar cycle period of 27 days.

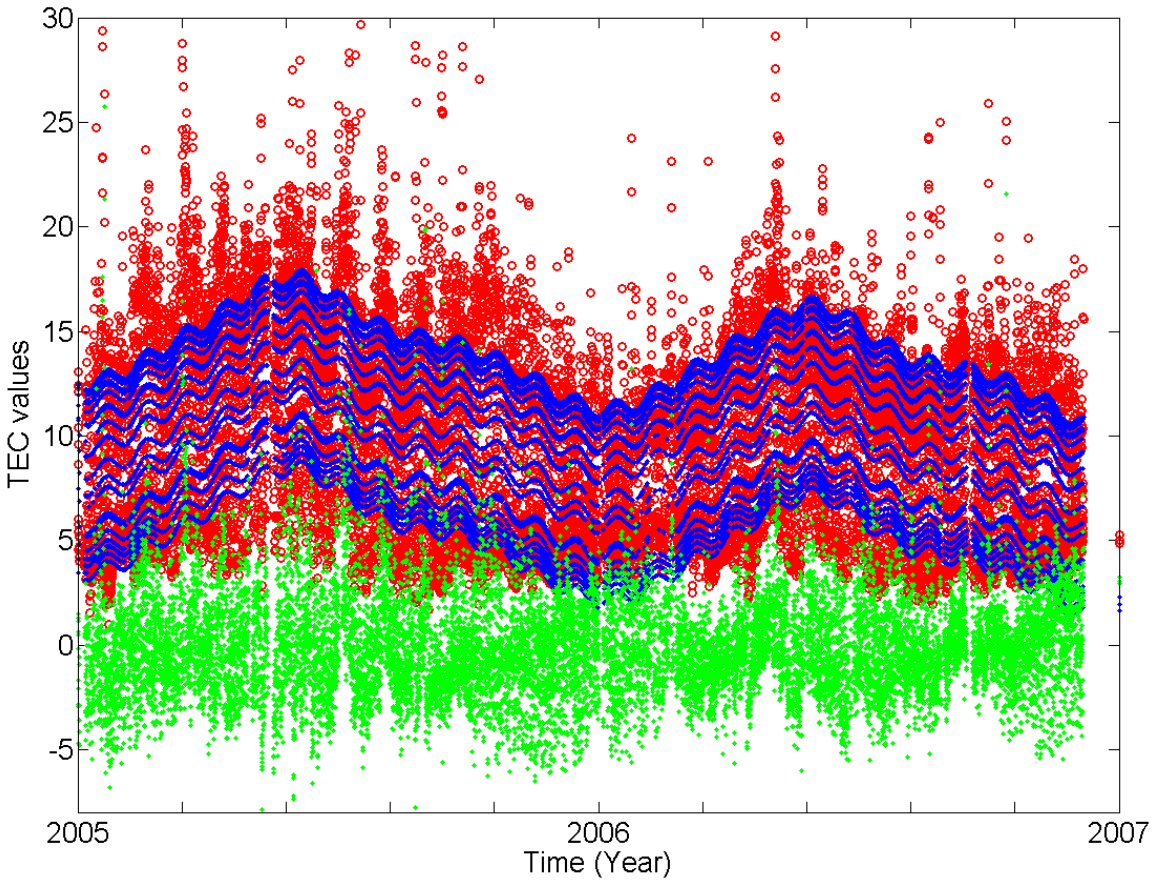

Figure 7. TEC values (red circles), least-squared fit using a set of harmonic functions (blue dots) and residuals (green dots) in 2005 and 2006.

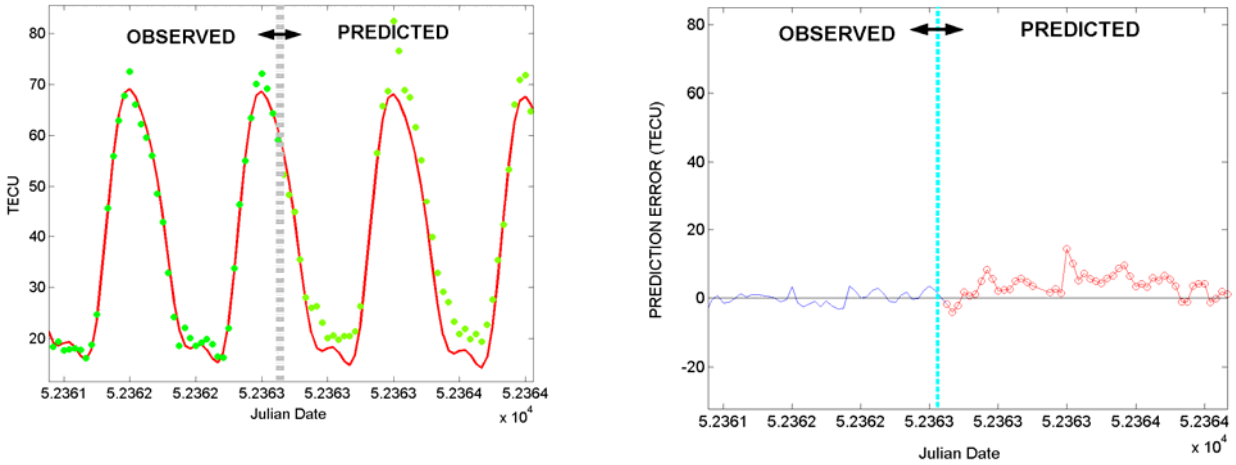

Figure 8. Prediction of TEC using LS-HE (left); green dots are the data set used for least-squares fit using diurnal, semi-diurnal and tri-diurnal signals, and red dots represents the original observations compared with predicted values of the blue solid line. The least-squares and predicted residuals are shown in the right frame.

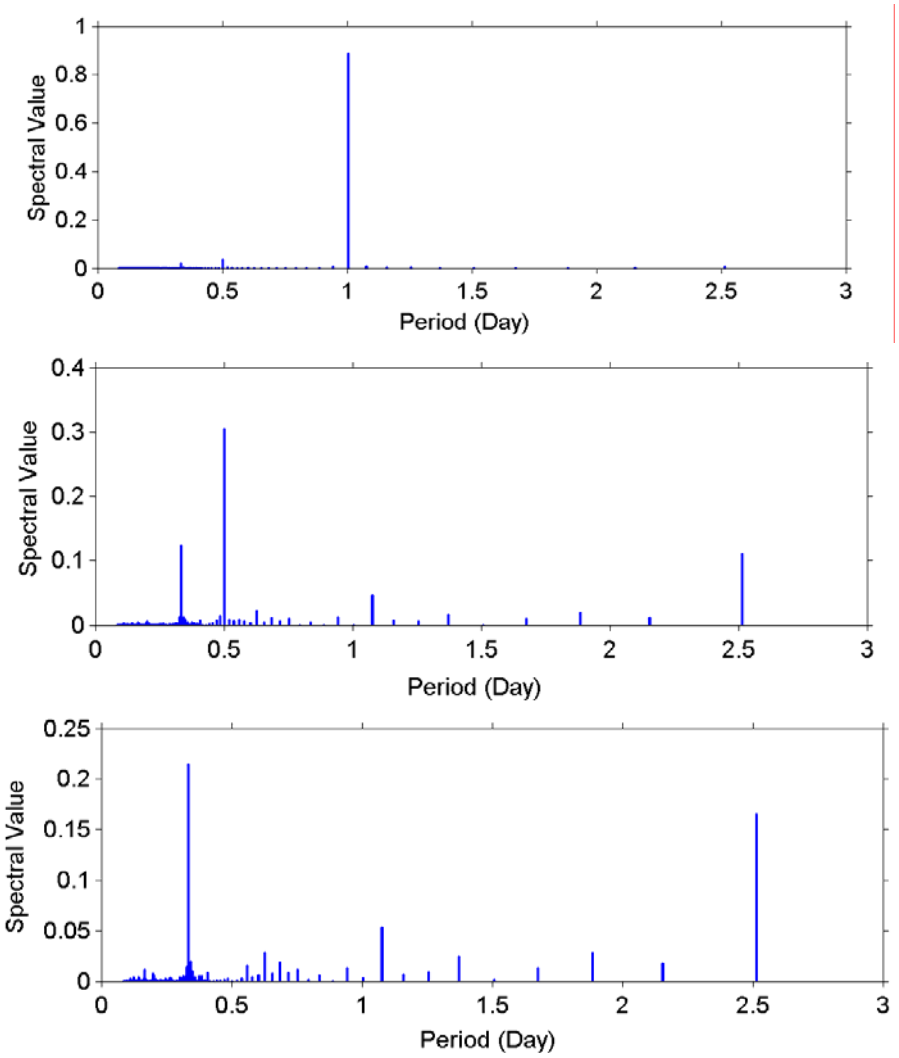

Figure 9. Least-squares spectrum for data used in Fig. 8 (top); spectrum for the same data after removing diurnal (1-day) period (middle); spectrum for the same data after removing both diurnal and semi-diurnal signals.

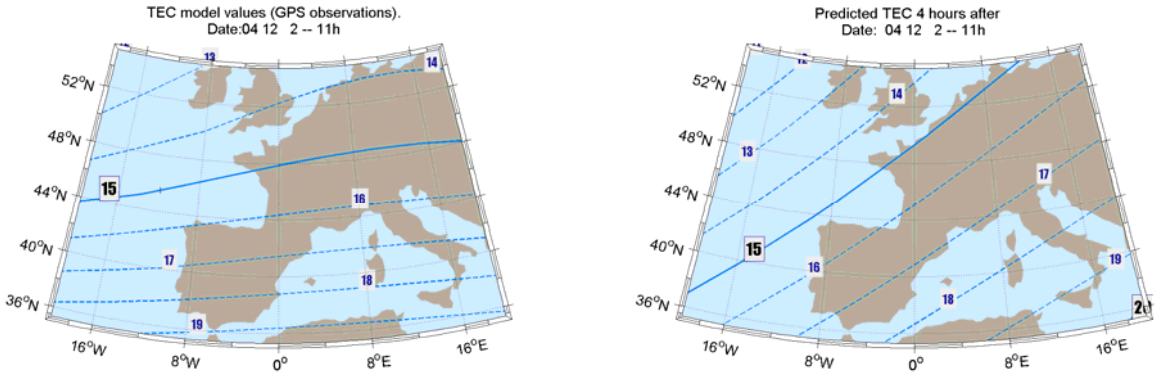

Figure 10. Local ionospheric prediction.

6 CONCLUSION AND RECOMMENDATIONS

In this study in addition to the detection of the dominant periods (mainly daily, semidiurnal, tridiurnal, seasonal and solar cycle variations) present in the total electron content of the ionosphere, we investigated the possible underlying physical interpretation. A linear trend along with a set of harmonic functions was considered. The dominant components are used for the harmonic estimation procedure. Based on the harmonic functions, the model was applied for long term (several days) predictions. The efficiency of the model degrades with increasing the prediction time. It is therefore advisable to use such a prediction model for only a few hours and the results are much better than the standard Klobuchar model. A prediction grid was proposed to expand the prediction to a 2D domain by application of the method to a regular grid. Real time users of the network with single frequency GPS receivers may use such gridded data to mitigate ionospheric error. Further investigation of the underlying physical interpretation of the dominant peaks is recommended.

RRFERENCES

Abbasi, M., 1999, Comparison of Fourier, least-squares and wavelet spectral analysis methods, tested on Persian Gulf tidal data. MSc thesis, Surveying Engineering Department, K.N. Toosi University of Technology, Tehran, Iran.

Amiri-Simkooei, A. R., 2007, Least-squares variance component estimation: theory and GPS applications. PhD thesis, Mathematical Geodesy and Positioning, Faculty of Aerospace Engineering, Delft University of Technology, Delft, Netherlands.

Artru, J., 2001, Observations au sol ou par satellite et modélisation des signaux ionosphériques post-sismiques. PhD thesis, Institut de Physique du Globe de Paris, Paris, France.

Asgari, J. and Harmel, A., 2005, Least squares spectral analysis of GPS derived ionospheric data. The ION National Technical Meeting, Jan.24-26 San Diego, California.

Balan, N., Kawamura, S., Nakamura, T. et al, 2006, Simultaneous mesosphere-lower thermosphere and thermospheric F region observations using middle and upper atmosphere radar. JGR DOI:10.1029/2005JA011487.

Bossolasco, M. and Elena, A., 1960, On the lunar semidiurnal variation of the D and F2 layers, Pure and Applied Geophysics, **46**(1): 167-172.

Craymer, M., 1998, The Least Squares Spectrum, its inverse iransform and autocorrelation function: Theory and some applications in geodesy. PhD thesis, Department of Civil Engineering, University of Toronto, Canada.

Dach, R., Hugentobler, U., Fridez, P., Meindl, M., 2007, User manual of the Bernese GPS Software Version 5.0. Astronomical Institute of the University of Berne, Berne, Switzerland.

Hernández-Pajares, M., Juan, J. M., Sanz, J. and Colombo, O. L., 2000, Application of ionospheric tomography to real-time GPS carrier-phase ambiguities resolution, at scales of 400-1000 km and with high geomagnetic activity. Geophysical Research Letters, **27**(13), 2009-2012.

Jain, S., Vijay, S. K. and Gwal, A. K., 1996, An empirical model for IEC over Lunping. Advances in Space Research, **18**, 263–266.

Le Mouël, J. L., Shnirman, M. G. and Blanter, E. M., 2007, The 27-day signal in sunspot number series and the solar dynamo. Solar Physics, **246**, 295-307.

Klobuchar, J. A., 1987, Ionospheric time-delay algorithm for single-frequency GPS users, IEEE Trans. Aerosp. Electron. Syst., **23**(3), 325–331.

Mansillaa, G. A., Mosertc, M. and Ezquera, R. G., 2005, Seasonal variation of the total electron content, maximum electron density and equivalent slab thickness at a South-American station. Journal of Atmospheric and Solar-Terrestrial Physics **67**, 1687–1690.

Memarzadeh, Y., 2009, Ionospheric modeling for precise GNSS applications. PhD thesis, Delft University of Technology, Netherlands Geodetic commission, Publication on Geodesy, 71.

Oliveira, A. B. V. and Walter, F., 2005, Ionospheric equatorial anomaly studies during solar storms, URSI-GA2005, New Delhi, India.

Oyekola, O. S. and Akinrimisi, J., 2006, Tidal forcing variability on F-region parameters at the equatorial ionosphere. 36th COSPAR Scientific Assembly, Beijing, China.

Pi, X., Mendillo, M., Fox, M. W. and Anderson, D. N., 1993, Diurnal Double Maxima Patterns in the F Region Ionosphere: Substorm-Related Aspects. JGR 98(A8): 13,677-13,69.

Pagiatakis, S. D., 1999, Stochastic significance of peaks in the least-squares spectrum. J. Geodesy. **73**(2), 67-78.

Schaer, S., 1999, Mapping and Predicting the Earth's Ionosphere Using the Global Positioning System. Ph. D. Thesis, Astronomical Institute of the University of Berne, Switzerland.

Seeber, G., 2003, Satellite Geodesy, 2nd edition,Walter de Gruyter, Berlin, Germany.

Unnikrishnan, K., Balachandran, Nair, R. and Venugopal, C., 2002, Harmonic analysis and an empirical model for TEC over Palehua. Journal of Atmospheric and Solar-Terrestrial Physics. **64**. 1833-1840.

Vaníček, P., 1971, Further Development and Properties of the Spectral Analysis by Least Squares. Astrophysics and Space Science, **12**, 10-33.